Surface-Enhanced Raman Spectroscopy of Bacteria and Pollen

ATANU SENGUPTA, MARY L. LAUCKS, and E. JAMES DAVIS*

Department of Chemistry, Box 351700, University of Washington, Seattle, Washington 98195-1700; and Department of Chemical Engineering, Box 351750, University of Washington, Seattle, Washington 98195-1750

A technique for distinguishing biological material based on surface-enhanced Raman scattering (SERS) is reported in this work. Of particular interest is biological material that can be airborne. Silver colloidal particles with diameters in the range 10 to 20 nm and with a characteristic ultraviolet–visible (UV-VIS) absorption band at 400 nm were used to obtain SERS spectra of *Escherichia coli*, *Pseudomonas aeruginosa*, and *Salmonella typhimurium* bacteria and a number of tree and grass pollens (*Cupressus arizonica* (cypress), *Sequoia sempervirens* (redwood), *Populus deltoides* (cottonwood), *Poa pratensis* (Kentucky bluegrass), and *Anthoxanthum odoratum* (sweet vernal grass)). While differences in the SERS spectra among the bacteria were small, we found that the pollen spectra we analyzed could readily be distinguished from the bacteria spectra, and there were significant differences between pollen from different families. In order to obtain reproducible results, we studied the parameters controlling the interaction between the analyte and the nanoscale metallic surface. Our results show that the volume ratio of analyte to colloidal particles must be within a narrow range of values to optimize the signal-to-noise ratio of the SERS spectra and minimize the fluorescence from the analyte. Also, we found that the time-dependent behavior of colloidal/bacterial suspensions (or adsorption rate of the silver colloid particles on the bacteria) is strongly dependent on pH, density of bacteria in solution, and even, to some extent, the type of bacteria.

Index Headings: **Bacteria; Bio-aerosols; Pollen; Surface-enhanced Raman spectroscopy; SERS.**

INTRODUCTION

Rapid identification of bacteria and other airborne biological species is increasingly important because of the threat of bio-terrorism. Conventional off-line techniques for the identification of bacteria by eluting bacteria from filters and incubating them in a suitable growth medium do not provide rapid identification and response. Laser-induced fluorescence has been explored for real-time on-line discrimination between biological and non-biological aerosols,[1–4] but Pan et al.[2] pointed out that ''The problem of using fluorescence to classify atmospheric bioaerosols is challenging because (1) there are so many possible types of biological aerosol particles, (2) differences between emission spectra of highly purified bacterial or protein samples may be small (spectra may be dominated by a small number of primary fluorophores, e.g., aromatic amino acids, reduced nicotinamide compounds, and flavins), (3) differences may depend on growth conditions, the atmospheric environment (temperature, humidity, sunlight, etc.), and other factors, and (4) naturally occurring biological aerosols may be mixtures of several types of particles and compounds.'' Fluorescence discrimination between bacteria such as *Bacillus thuringiensis* and *Bacillus subtilis* is not generally adequate because of the similarity in their spectra.[2]

An alternate approach to the detection of bioaerosols is the application of spontaneous Raman spectroscopy, but fluorescence due to the fluorophores common to many biological particles masks Raman spectra as shown for a variety of pollen particles by Laucks et al.[5] By illuminating pollen particles using a near-infrared (NIR) wavelength (λ = 785 nm) they obtained Raman spectra without fluorescence. Sengupta et al.[6] demonstrated for bacteria that fluorescence can be quenched and strong Raman scattering can be obtained using surface-enhanced Raman scattering (SERS). This was accomplished by mixing a bacterial suspension with a colloidal suspension of silver particles prepared following a standard borohydride reduction recipe.[7] They made measurements of aerosolized bacteria as well as aqueous suspensions of bacteria. A commercial nebulizer was used to aerosolize the bacteria from an aqueous suspension before collecting the aerosolized stream in a cuvette filled with colloid.

Experiments with *Escherichia coli*, *Pseudomonas aeruginosa*, and *Salmonella typhimurium* showed that the volume ratio of bacteria (the analyte) to colloidal particles must fall within a certain range in order to maximize the signal and quench the fluorescence. Because bacterial cell walls have amino acids as building blocks, spectra of individual amino acids were obtained to interpret the more complicated bacterial spectra. Their spectra look roughly similar over a wide range of Raman shifts, but there are some differences in the region 500–1100 cm^{-1}, a result also reported by Bronk and Efrima.[8]

Surface-enhanced Raman scattering seems to be a promising technique for obtaining useful spectra of biological species. Recently, Alexander et al.[9] published the use of near-infrared SERS to obtain spectra of single optically trapped bacterial spores in an aqueous medium. They used ~60 nm diameter gold colloidal particles bound to 3-aminoproplytriethoxysilane-derivatized glass as the SERS substrate. They reported spectra for two different strains of single *Bacillus stearothermophilus* spores and found a relatively modest enhancement of order 10^2. Jarvis and Goodacre[10] used silver colloidal nanoparticles to characterize bacteria by SERS and they observed subtle quantitative differences in ''raw'' spectra of *E. coli* isolate and *Enterococcus sp.* (ENTC90) isolate.

The SERS technique requires that analyte groups be in close proximity to a nanoscale metallic surface, and the magnitude of enhancement depends on the distance of the groups from the metallic surface, decaying with in-

Received 26 January 2005; accepted 2 May 2005.

* Author to whom correspondence should be sent. E-mail: davis@cheme.washington.edu.

0003-7028/05/5908-1016$2.00/0

© 2005 Society for Applied Spectroscopy

creasing distance from the active surface.[11,12] Therefore, a better understanding of the parameters controlling the interaction between analyte and nanoscale metallic surface is needed to optimize the SERS detection system.

The purposes of the work reported in this paper were to extend the work of Sengupta et al. to other airborne biological particles (pollen), to examine the rate of development of SERS, and to investigate the mechanisms controlling the analyte-to-colloid ratio needed to maximize SERS. The ultimate goal is to develop a compact detector based on SERS to monitor airborne biological samples. Since air can contain biological species such as pollen as well as bacteria, we conducted SERS studies of pollens to determine if they can be discriminated from common bacteria using their spectral fingerprints.

Prior to this study, our SERS investigations of bacteria indicated that, in addition to the volume ratio of bacterial suspension to colloid suspension, the SERS signal depends on the age of the colloid/analyte mixture. Podstawka et al.[13] recently reported similar results for SERS spectra of amino acids and their homodipeptides adsorbed on colloidal silver. They suggested that the silver colloid particles aggregate with time and that larger clusters cause the analyte group to move or reorient with respect to the colloid particle. In fact, by inspecting the SERS spectra, Podstawka et al. found evidence that the homodipeptide was bound to the silver surface, first through a carboxyl group and then, after more than 3 hours, through the N-termini group, indicating that a complete re-orientation with respect to the silver surface had occurred. It should be noted that in the experiments of Podstawka et al. the analyte was much smaller than the silver colloid particles, whereas in the current work, the silver colloid particles are much smaller than the bacteria and pollen. However, the interactions between surface groups and the colloidal silver are analogous in some sense.

EXPERIMENTAL

Sengupta and his co-workers[6] investigated both aerosolized and non-aerosolized bacteria. The experimental system for non-aerosolized bacteria discussed by those authors was used in this work, so only a brief description of the equipment is needed here. The biological particles were injected into a cuvette containing a nanocolloidal suspension of silver. The 1.0 cm $\times$ 1.0 cm $\times$ 4.5 cm optical glass cuvette was illuminated using the beam from an argon-ion continuous wave (CW) laser operating at a wavelength of 514.5 nm. Light scattered at 90° from the beam by the bioanalyte/silver colloid suspension was focused on the slit of a 500 mm focal length single pass Acton SpectraPro-500I monochromator with a grating turret permitting dispersions of 300, 1200, and 2400 lines/mm. A Kaiser Optical Systems SuperNotch-Plus holographic filter was placed in front of the spectrometer to remove the laser line. The spectrum was recorded using a Princeton Instruments back-illuminated, liquid nitrogen-cooled 1340 $\times$ 100 pixel array charge-coupled device (CCD) camera. The laser beam power at the cuvette was typically ~100 mW. The exposure time was usually 120 s.

Three types of experiments were performed. In the first set of experiments 70–100 μL of an aqueous bacterial suspension were added to different volumes of freshly prepared silver colloid to determine the optimum volume ratio to maximize the Raman scattering. Bacterial samples were incubated for 17 hours in a Luria broth growth medium and grown until they reached their stationary growth stage. This corresponded to a concentration in the range of 10^7–10^8 cfu/mL. The optical density at 600 nm (OD600) was measured for the samples and varied between 0.6 and 3.4.

The bacteria investigated included three types (*Salmonella typhimurium, Pseudomonas aeruginosa,* and *Escherichia coli*) and three strains of *E. coli. E. coli* and *Salmonella* are in the family Enterobacteriacae, and *Pseudomonas* is a Proteobacteria in the family Pseudomonadaceae. The members of a family (a category of related plants or animals above a genus and below an order) can be expected to have some chemical similarity.

In the second set of experiments the effect of pH on the dynamics of the silver/bacteria interaction process was explored. In this case 100 μL of an *E. coli* suspension (OD600 = 3.4) was mixed with 5 mL of silver colloid for pH 3.25, 8.0, and 9.74. The pH was controlled by the addition of hydrochloric acid and sodium hydroxide. The growth of the major peak at 1355 cm^{-1} over time was used to follow the adsorption dynamics. This peak represents the CH– and $–CH_2$ bending and wagging deformations from protein groups,[14] which are expected to be present on the bacterial cell wall. The growth of this peak over time gives some indication of the adsorption dynamics of the silver particles on the wall surface.

The third set of experiments measured SERS for a variety of pollen, including *Cupressus arizonica* (cypress), *Sequoia sempervirens* (redwood), *Populus deltoides* (cottonwood), *Poa pratensis* (Kentucky bluegrass), and *Anthoxanthum odoratum* (sweet vernal grass) pollen. The pollen measurements were made using the same silver colloid suspension as for the bacteria. All the pollen samples were obtained from Bayer Corporation (Spokane, WA). A dilute (transparent) suspension of the pollen of undetermined concentration was mixed with the silver colloid suspension and inserted into the cuvette for the SERS experiments.

RESULTS AND DISCUSSION

Analysis of Bacteria. The earlier results of Sengupta et al. indicate that there is a window in the ratio of silver particles to biological particles within which SERS is effective. Presumably, only certain groups on the bacterial cell wall interact with the silver nanoparticles. To investigate this effect, we varied the number density ratio by controlling the volume ratio of the bacterial aqueous suspension to the colloidal suspension.

Figure 1 shows SERS spectra of MC4100 *Escherichia coli* (OD600 = 3.4) for different volume ratios, VR, where VR = (volume of the bacterial suspension)/(volume of the silver colloidal suspension). The spectra have been normalized with respect to the water peak at 1635 cm^{-1} and then shifted so that the baselines are all zero at 1827 cm^{-1}. For all of the spectra the band at 1635 cm^{-1} is clearly seen. This is associated with HOH bending,[15] and it overlays an amide band in that region.[14] The broad envelope in the low frequency region (<1000 cm^{-1}) can

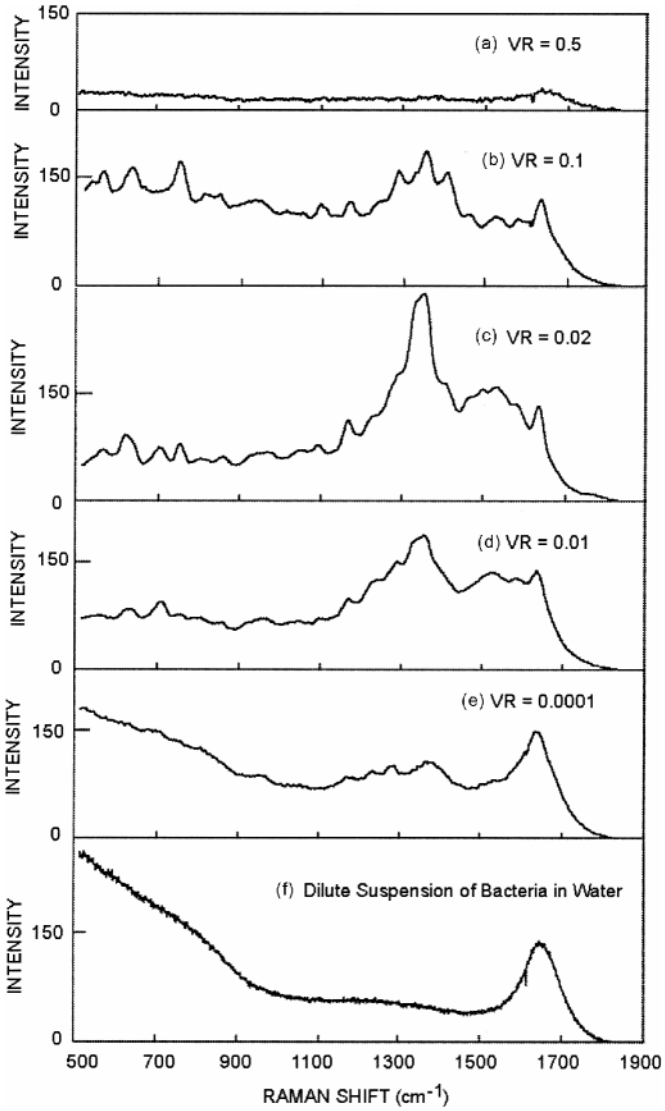

FIG. 1. SERS spectra of MC4100 *E. coli* (OD600 = 3.4) at different volume ratios (VR). The intensity on the ordinate axis is in counts per second.

be attributed to librational modes of water, that is, rotational oscillations of the water molecules.[16] Moskovits and Michaelian[15] showed that the librational envelope extends from about 200 cm^{-1} to ν_2 (the bending mode) for HOH, HOD, and DOD. Their Raman data for water are very similar to Fig. 1f over the region 500–1800 cm^{-1}. At the lowest concentrations of bacteria, Figs. 1e and 1f, the librational envelope is a dominant feature in the region 500–900 cm^{-1}. The librational envelope and the band at 1635 cm^{-1} are also seen in the spectrum of the colloidal suspension in the absence of bacteria (not shown).

Figure 1 demonstrates the existence of a narrow window within which we can see large signal enhancement. Strong signal enhancement was observed for VR in the range 0.01–0.05, and the maximum signal enhancement was achieved for VR = 0.02. At VR = 0.5, the enhancement is low because there are not enough silver particles in contact with the relevant groups on the bacteria due to the low concentration of silver particles in the suspension. For VR = 10^{-4} the spectrum is clearly affected by the librational band of water. The spectra in Fig. 1, except for Fig. 1f, were obtained by diluting a suspension of *E. coli*, grown to its stationary stage, by a factor of 10^{-2} and then mixing them with the colloidal suspension using the volume ratios indicated in the figure. If the initial concentration of bacteria was 10^8 cfu/mL, the first dilution yielded 10^6 cfu/mL, and the final mixing with the colloidal suspension yielded a concentration of only 10^2 cfu/mL. It appears that the low intensity at VR = 10^{-4} is due to the fact that very few bacteria were in the small volume of the suspension illuminated by the laser beam. It is not likely that the low intensity was due to a reduction in SERS enhancement resulting from the formation of larger colloidal particles because no formation of aggregates was observed (by a change in color).

The role of particle aggregation in the enhancement of Raman scattering for small molecules has been studied by Kerker et al.[17] and Wetzel et al.[18] among others. According to these studies, the addition of analyte induces a red shift of the silver plasmon band (originally at 400 nm) and causes a broad secondary band to form at a longer wavelength (500–600 nm). Creighton et al.[19] found that this second extinction band is responsible for further signal enhancement of pyridine molecules due to strong resonance coupling with the exciting wavelength. In his excellent review of SERS, Moskovits[12] discussed the role of particle size and the interaction of surface plasmons with the excitation wavelength. Large enhancements are expected when the excitation frequency is near surface-plasmon resonance conditions. Particle aggregation changes the particle size distribution and thus shifts the plasmon resonance condition towards longer wavelengths. Also, recent investigations have shown that the signal is enhanced at certain hot spots between individual particles in an aggregated cluster.[20,21] The local field is typically enhanced by a few orders of magnitude at this junction.[22] This is the basis for possible application of SERS in detecting single molecules. The field is advancing rapidly, and there are reports of single molecule detection using this technique.[23,24]

Measurements of the ultraviolet–visible (UV-VIS) absorption of silver colloidal solutions were made in addition to our Raman measurements to determine the position of the plasmon absorption bands and their effects on Raman signals. We also investigated the time dependence of particle aggregation induced by biological species, such as bacteria and pollen, whose sizes are several orders of magnitude greater than those of small molecules typically investigated using SERS. The average size of the colloidal particles used in our work was 10–20 nm with a characteristic UV-VIS absorption band at 400 nm.

Figures 2 and 3 present the time-dependent UV-VIS absorption data and SERS spectra, respectively, for *Escherichia coli* grown to OD600 = 3.4 in a silver colloidal suspension. Figure 2 shows the development of a secondary absorption band at ~510–550 nm and is most likely the result of a change in the particle size distribution over time. The development of this band is due to the formation of aggregated silver clusters. These results support the previous findings of Zeiri et al.,[25] which suggest that silver colloid particles bind only to certain specific groups on the bacterial cell wall (e.g., flavins). The line labeled ''blank colloid'' refers to an experiment in

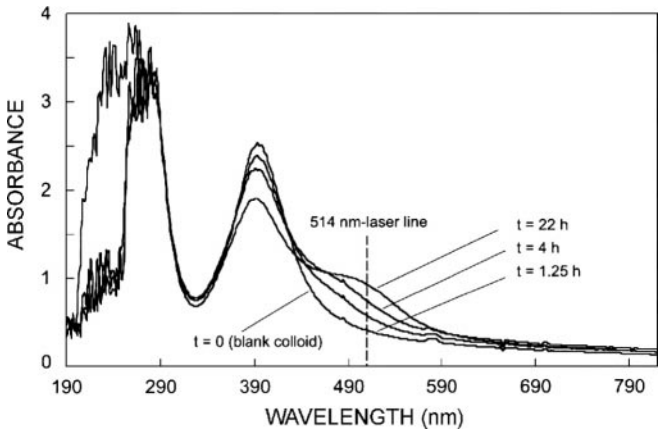

FIG. 2. Time-dependent UV-VIS results performed to investigate the particle aggregation behavior induced by adding 100 μL of MC4100 *E. coli* to 5 mL of the silver colloidal solution (VR = 0.02).

which no bacteria were present in the colloidal suspension.

Figure 3 shows the time-dependent evolution of the Raman spectrum for the same sample of *E. coli* mixed with a silver colloidal suspension. Since the background varied from run to run we adjusted the baselines of the spectra to give zero intensity at a Raman shift of 1827 cm^{-1}. This yielded essentially the same intensity for each water peak at 1635 cm^{-1}. The growth of the major band of the Raman spectrum (1300–1500 cm^{-1}) over time is clearly illustrated in Fig. 3. As can be seen by comparing Figs. 2 and 3, the secondary absorption band in the UV-VIS spectra and the SERS band evolve over a similar time scale, indicating that plasmon resonance coupling is an important mechanism in the Raman signal enhancement.

The results shown in Fig. 3 indicate that the major peaks of the Raman spectrum appeared within a few minutes, and then the intensity increased relatively slowly for several hours. This could be due to a relatively slow rate of attachment of colloidal particles to active sites on the bacteria. Subtle structural differences on the surfaces of different microorganisms are expected to result in different binding rates with metallic particles.

A variety of SERS measurements were made for three strains of *E. coli* (RW193, BL21, and UT1440), for LT2 *Salmonella,* and for PAO1 *Pseudomonas,* and four sets of spectra are compared in Fig. 4. The SERS spectrum for UT1440 *E. coli* is identical to the spectrum for BL21 *E. coli,* so it is not shown. All of the spectra are similar in the region >1200 cm^{-1}, and the *E. coli* spectra differ somewhat from those of *Salmonella* and *Pseudomonas* in the region <900 cm^{-1}. Additional discussion of SERS spectra for bacteria is provided below.

To explore the parameters affecting the attachment or ''binding'' rate, we used the peak height changes of the major peak (at 1355 cm^{-1}) over time. Adsorption rate studies showed that the adsorption characteristics are sensitive to the concentration of bacteria. In Fig. 5 the normalized peak height at 1355 cm^{-1} (relative to the water peak at 1635 cm^{-1}) is plotted as a function of time for different optical densities of LT2 *Salmonella typhimurium.* For the more dilute bacterial suspensions (OD600 < 2) the peak height increased with time, but at higher

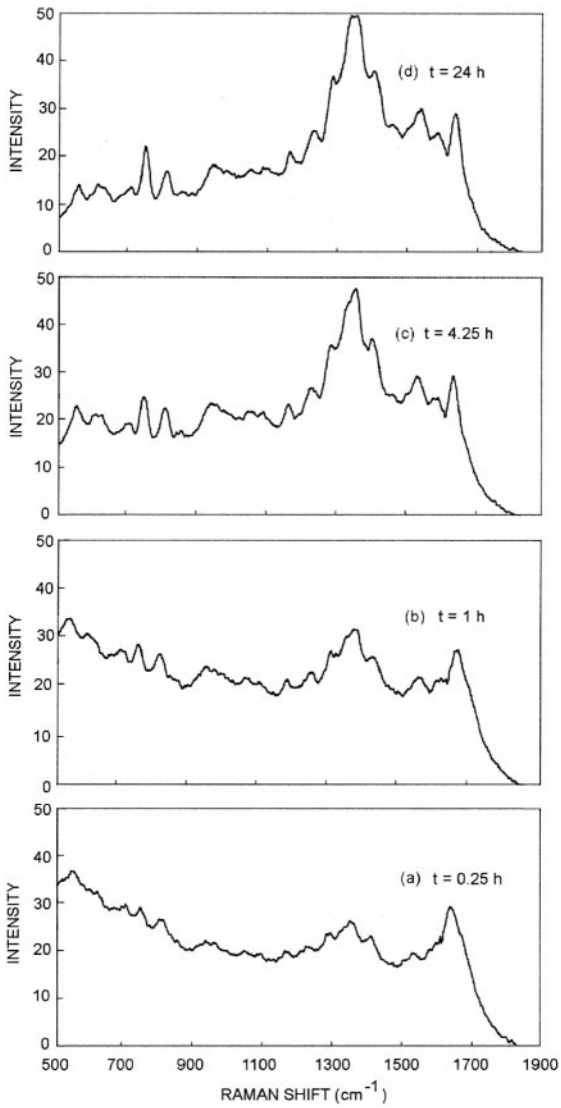

FIG. 3. Time-dependent SERS for MC4100 *E. coli* (OD600 = 3.4) mixed with silver colloid for VR = 0.02. The intensity on the ordinate axis is in counts per second.

optical densities (OD600 > 2) the peak height decreased with time. At lower concentrations it is postulated that the colloidal particles slowly aggregated, and the enhancement increased as the absorption band shown in Fig. 2 broadened. At the higher concentrations the colloidal particles aggregated more rapidly and reduced the Raman enhancement by lowering the number of silver particles available for binding to surface groups. In the experiments with OD600 > 2, we saw evidence of silver precipitation and color change.

In addition, we found that the adsorption dynamics vary for the different bacteria species; MC4100 *Escherichia coli* adsorbs faster than *Pseudomonas aeruginosa.* The rates of change of peak height for BL21 *Escherichia coli* and LT2 *Salmonella typhimurium* were nearly the same and were intermediate to the other two species. The peak height changes were also found to be different for different strains of the same bacterial species.

The adsorption characteristics are also expected to be sensitive to the surface charge or zeta potential of the colloidal particles. The literature indicates that metal col-

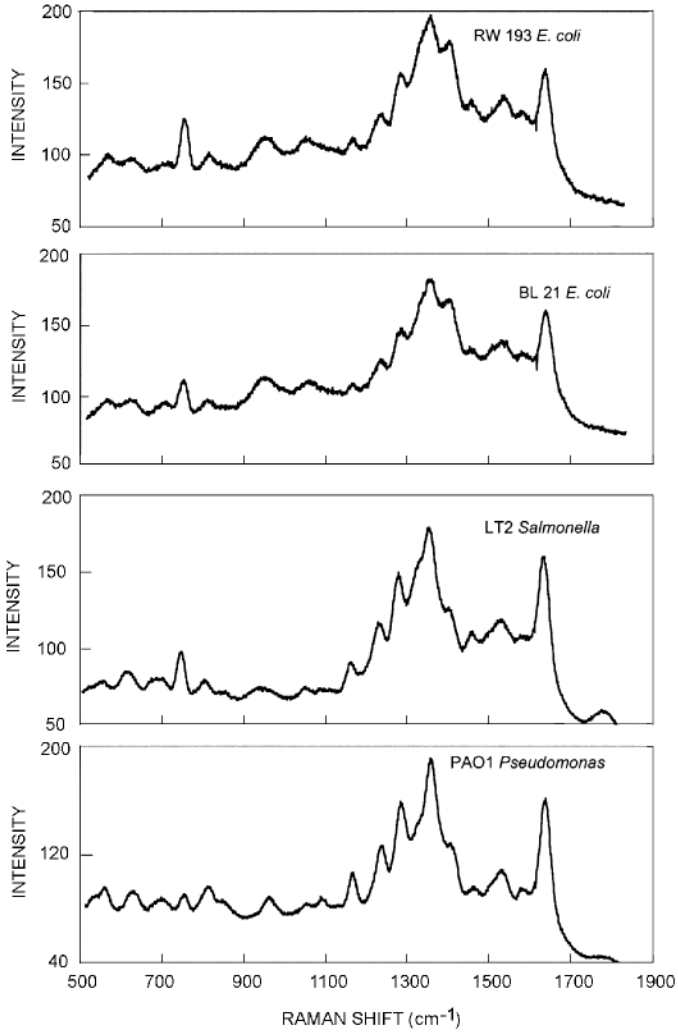

FIG. 4. SERS spectra for bacteria.

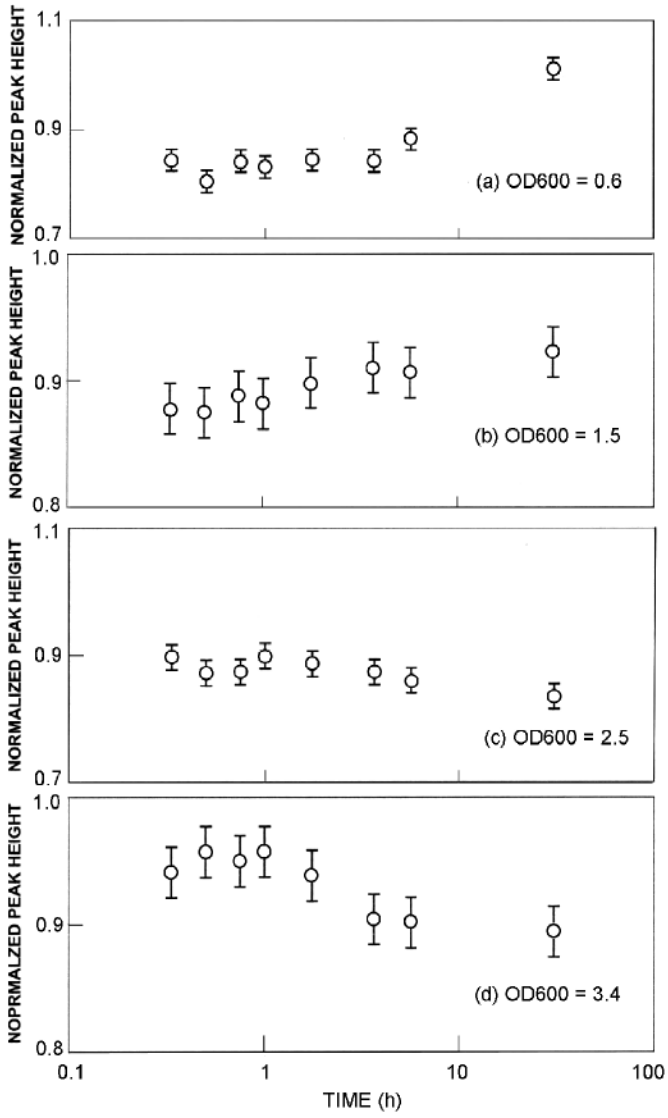

FIG. 5. The normalized peak height at 1355 cm^{-1} as a function of time for different concentrations (OD600) of LT2 *Salmonella* with VR = 0.02.

loids have a negative zeta potential at pH = 8.[26] The colloidal stability and aggregation characteristics depend on the surface charge. Dou et al.[26] observed that SERS intensity of the amino acid glycine dramatically varied with a change in pH and found that intensities sharply increased as the pH was changed from basic to acidic. They attributed this to the fact that, under acidic conditions, positive charges are developed on the amino acid backbone due to the protonation of the NH_2 group, which increases the binding affinity of the amino acid groups to the negatively charged colloidal particles.

To increase the rate of adsorption and decrease the time to maximum enhancement, we measured the time-dependent spectra for MC4100 *E. coli* (OD600 = 3.4) as a function of pH (pH = 3.25, 8, and 9.74). The rate of evolution was found to be much faster at pH = 3.25 than under basic conditions, and the spectrum in the region 1200–1700 cm^{-1} reached a steady state in approximately 10 min, as shown in Fig. 6.

In the region <1000 cm^{-1} the intensity continued to increase with time and began to show an increase in the background in the region 500–900 cm^{-1} also seen in the spectra of Figs. 1e, 1f, 3a, and 3b. Ooka and Garell[27] reported similar results in the SERS spectra of 3,4-dihydroxyphenylalanine (DOPA) containing peptides, usually found in adhesive protein of the marine mussel, *Mytilus edulis.* According to the authors this background was most likely due to the fluorescence of impurities, but in our case the background can be attributed to the broad librational envelope of water discussed above.

The time evolution of the background in the region 500–900 cm^{-1} suggests that under acidic conditions and in the presence of chloride ions the colloidal suspension was unstable, and we observed aggregated particles precipitating out. That reduced the number of colloid particles available for binding, and consequently there were not enough silver particles to produce a large enhancement.

Practically no binding occurred at pH = 9.74, but at pH = 3.25 the enhancement was found to be short-lived and was followed by a gradual decay of the SERS peak heights, as shown in Fig. 7. Although we achieved much faster analysis, the colloid instability makes it undesirable to operate at low pH.

Analysis of Pollen. As found in previous work,[6] dif-

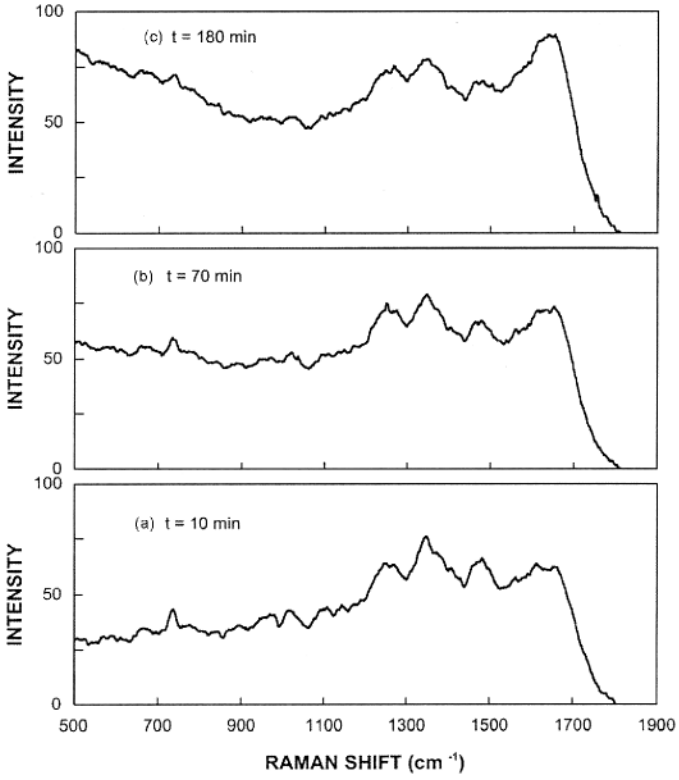

FIG. 6. SERS spectra for *E. coli* (OD600 = 3.4) in a silver colloid suspension at pH = 3.25. The intensity on the ordinate axis is in counts per second.

ferent strains of the same bacteria species and even different species of bacteria show relatively small differences in their SERS spectra, but in this work we have found that bacteria show significant differences compared with the pollen we studied. In addition spectral differences between these pollen species are significant.

The differences between pollen species are illustrated in Fig. 8, which shows SERS spectra for Kentucky bluegrass, sweet vernal grass, redwood, and cypress. A SERS spectrum for cottonwood pollen is presented in Fig. 9. In these figures, all spectra have been normalized relative to the water peak at ~1635 cm^{-1}.

Redwood and cypress belong to the family Cupressaceae, sweet vernal grass and Kentucky bluegrass belong to the family Poaceae, and cottonwood to the family Salicaceae. The bluegrass and sweet vernal grass spectra are similar, as might be expected of members of the same family. The redwood and cypress spectra are also similar, and the spectra of the two families show distinctive differences in the region 1100–1300 cm^{-1}. The cottonwood

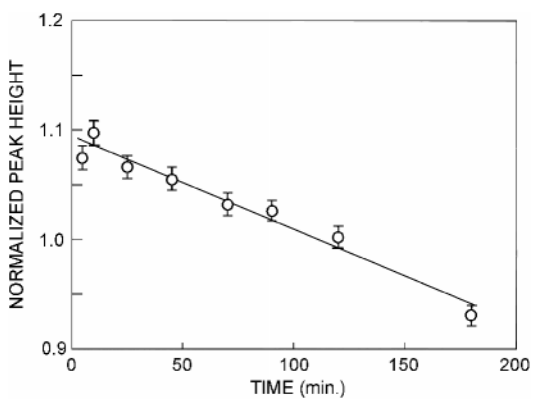

FIG. 7. Decay of the major peak (at 1355 cm^{-1}) in the SERS spectrum of MC4100 *E. coli* (OD600 = 3.4) for VR = 0.02 and pH = 3.25.

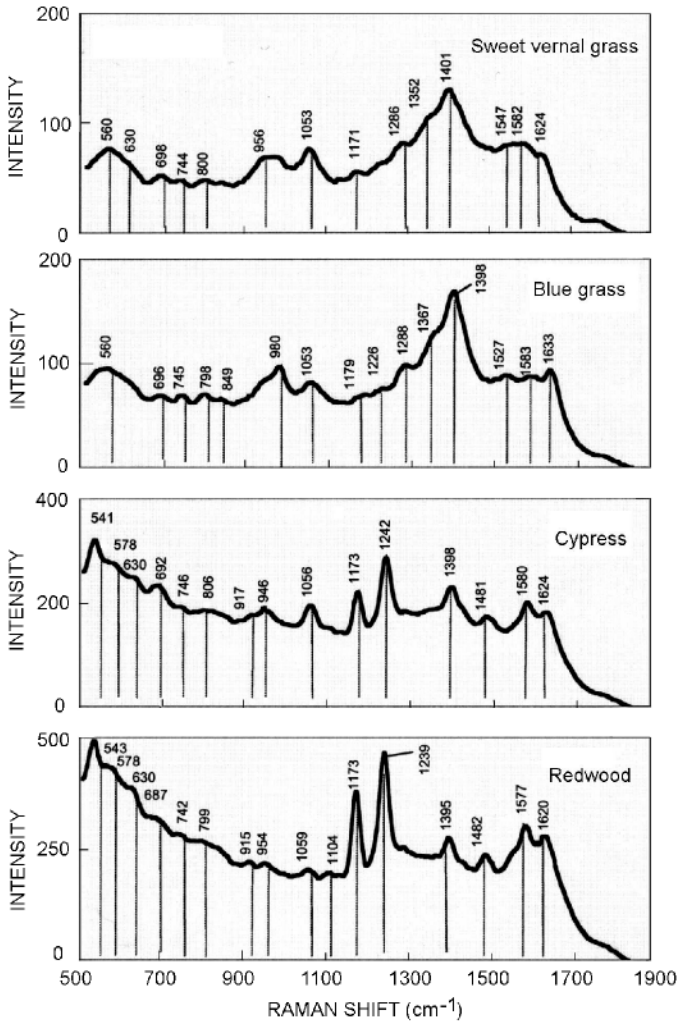

FIG. 8. SERS spectra for some grass and tree pollen. The spectra were normalized to the water peak at 1635 cm^{-1}.

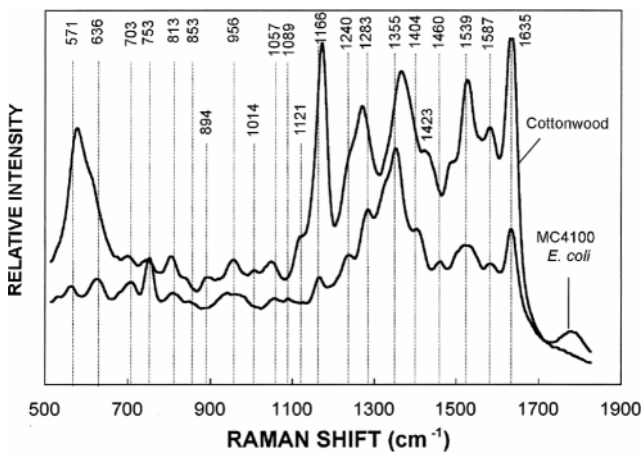

FIG. 9. Comparison of SERS results for MC4100 *E. coli* and cottonwood pollen.

TABLE I. Assignment of the peaks identified in Fig. 9 for MC4100 *E. coli* and cottonwood pollen. (Notation: b = broad, m = medium, s = strong, sh = shoulder, vw = very weak, w = weak.)

MC4100 *E. coli*	Cottonwood pollen	Tentative peak assignment
571 (m)		Carbohydrates[29]
	578 (s)	COO^- wag[30]
636 (s)		COO^- bend[30]
703 (m)	701 w)	adenine from flavin[28]
753 (s)	747 (w)	ring I deformation[28]
813 (m), 853 (vw),	806 (s), 846 (vw, sh) 894 (m)	different C–N stretch,[26–29] probably from tyrosine groups[26]
956 (s, b)	956 (s)	C–N stretch[30]
	1014 (vw)	C–N stretch from phenylalanine[29,30]
1057 (w), 1089 (w)	1049 (w)	Carbohydrates, C–C, C–O, –C–OH deformation[29]
	1121 (w, sh)	=C–C= (in lipids), C–N (protein)[9,14]
1166 (m)	1173 (s)	aromatic amino acids in proteins[14]
1240 (m, sh)	1240 (w, sh)	N–H, C–N, amide III[29]
1283 (m)	1274 (s)	=CH in plane (lipid) or amide III (protein)[14]
1355 (s)	1367 (s)	C–H bend (protein)[14]
1404 (s, sh)		COO^- symmetric stretch[30]
1460 (w)	1423 (w, sh)	CH_2 bend (protein, lipid)[14]
1539 (s, b)	1527 (s)	N–H, C–H bend, C=C stretch[28]
1587 (w)	1583 (w)	C=C (lipid)[29]
1635 (s)	1635 (s)	Water[15]

pollen spectrum shares similarities with both the grasses and the cypress and redwood pollen.

All of the pollen spectra have bands that can be attributed to flavins. Zheng et al.[28] published an extensive list of wavenumbers (cm^{-1}) and the assignment of Raman bands for reduced flavins in H_2O and D_2O. For example, they attributed the band at ~1390 cm^{-1} to the ring I mode.

There are relatively small differences between the sweet vernal grass and Kentucky bluegrass spectra; the three distinct peaks in the bluegrass spectrum in the region 1500–1640 cm^{-1} are absent in the sweet vernal grass spectrum, and the peak at 980 cm^{-1} in the bluegrass spectrum is not pronounced in the sweet vernal grass spectrum. Most of these small differences may be attributed to slightly different local environments for the same chemical groups.

The spectra for cypress and redwood are distinguished by large peaks near 540, 1173, and 1240 cm^{-1} and a minor peak near 1480 cm^{-1} that are not present in the two grass spectra. The only region in which the redwood spectrum can be distinguished from the cypress spectrum is between 1050 and 1120 cm^{-1}. Cypress has a moderately large peak at 1056 cm^{-1}, whereas redwood has two minor peaks at 1059 and 1104 cm^{-1}. The peaks near 540, 1056, and 1173 cm^{-1} have been attributed to carbohydrates,[29] while the 1240 cm^{-1} peak has been attributed to N–H, C–N, and amide III.[29]

The cottonwood spectrum has an extremely large peak at 578 cm^{-1} that has been attributed to the COO– wag,[30] but it does not have a peak at 541 cm^{-1}, which is present in both redwood and cypress. Cottonwood has a very small peak at 1240 cm^{-1} (attributed to N–H, C–N, and amide III[29]) unlike the dominant 1240 cm^{-1} peak in redwood and cypress. The cottonwood, redwood, and cypress spectra all contain large peaks at 1173 cm^{-1}, which have been attributed to aromatic acids in proteins.[14]

Comparison of Bacteria and Pollen. A detailed comparison of MC4100 *E. coli* and cottonwood pollen is presented in Fig. 9. In this figure, the spectra are shifted vertically for purposes of visualization, and lines are drawn centered on the major MC4100 *E. coli* peaks for reference. Table I shows tentative peak assignments for the *E. coli* and cottonwood peaks labeled in Fig. 9. Since our suspensions were all in deionized water, the large peaks at 1635 cm^{-1} are due to water and overlay any other peak at this Raman shift, such as the C=C (lipid) or amide I (protein) peaks. We are, therefore, justified in normalizing with respect to this peak. The spectra for dilute suspensions of bacteria and for the colloidal suspension without bacteria show this same peak.

The most striking differences between the *E. coli* spectrum and the cottonwood pollen spectrum are the much larger peaks at 578 cm^{-1}, 1166 cm^{-1}, and 1635 cm^{-1} in the cottonwood spectrum compared to the *E. coli* spectrum. The 755 cm^{-1} peak in the *E. coli* spectrum is much larger than the same peak in the cottonwood spectrum. The peaks at 571, 813, 1057, 1166, 1283, 1355, and 1404 cm^{-1} in the *E. coli* spectrum are shifted from the analog peaks in the cottonwood spectrum. There is a peak at 1460 cm^{-1} in the *E. coli* spectrum but not the cottonwood spectrum, and the cottonwood peaks at 894, 1014, 1121, and 1423 cm^{-1} are not found in the *E. coli* spectrum.

As can be seen in Table I, the relatively large peaks at 571 cm^{-1}, 1166 cm^{-1}, and 1635 cm^{-1} in the cottonwood spectrum can be attributed to carbohydrates,[29] aromatic amino acids in proteins,[14] and the C=C bond in lipids,[14] respectively. The cottonwood peak at 894 cm^{-1} can be assigned to a C–N stretch,[29,30] probably some moieties not found in *E. coli.* The cottonwood peak at 1014 cm^{-1} can be assigned to the C–N stretch from phenylalanine,[29,30] the 1121 cm^{-1} to =C–C= unsaturated fatty acids in lipids,[29] and the 1423 cm^{-1} peak to a CH_2 bend in protein or lipids.[14]

CONCLUSION

We have demonstrated that pollen and bacteria can be differentiated using surface-enhanced Raman spectra obtained from a suspension of nanocolloidal silver particles mixed with the bio-analyte. We have also shown that different families of pollens are distinguishable from each

other and from bacteria, but the differences are not pronounced within the same family. These results suggest that SERS is a satisfactory technique for differentiating pollen from bacteria and could form the basis of a detection system that indicates the presence of bacteria.

The detection and characterization of bacteria is sensitive to the volume ratio of colloidal particles to bacteria, and the time rate of change of the spectra is much greater at acidic pH than at basic pH due to instability of the silver colloid at low pH. These results suggest that binding of the silver particles to active sites on the biological particles is strongly affected by the charge states of the colloidal particles and the surface. At acidic pH and at higher volume ratios of colloid particles to bacteria, aggregation of the colloidal particles leads to relatively rapid deterioration of the Raman signal. These results identify some of the parameters that must be controlled to obtain reproducible results with SERS.

ACKNOWLEDGMENTS

The authors thank Professors Daniel T. Schwartz and François Baneyx for their interest and advice. Mirna Mujacic in Professor Baneyx's laboratory provided the bacterial samples and her contributions are highly appreciated. The authors also thank the National Science Foundation for Grant Number CTS-9982413, the University of Washington/PNNL Joint Institute for Nanotechnology, and the University of Washington Center for Nanotechnology for their financial support.

1. R. G. Pinnick, S. C. Hill, P. Nachman, G. Videen, G. Chen, and R. K. Chang, Aerosol Sci. Technol. **28,** 95 (1998).
2. Y. L. Pan, S. Holler, R. K. Chang, S. C. Hill, R. G. Pinnick, S. Niles, and J. R. Bottiger, Opt. Lett. **24,** 116 (1999).
3. M. Seaver, J. D. Eversole, J. J. Hardgrove, W. K. Cary, and D. C. Roselle, Aerosol Sci. Technol. **30,** 174 (1999).
4. R. G. Pinnick, S. C. Hill, Y. L. Pan, and R. K. Chang, Atmos. Environ. **38,** 1657 (2004).
5. M. L. Laucks, G. Roll, G. Schweiger, and E. J. Davis, J. Aerosol Sci. **31,** 307 (2000).
6. A. Sengupta, M. L. Laucks, N. Dildine, E. Drapala, and E. J. Davis, J. Aerosol Sci. **36,** 651 (2005).
7. R. Keir, D. Sadler, and W. E. Smith Appl. Spectrosc. **56,** 551 (2002).
8. B. V. Bronk and S. Efrima, J. Phys. Chem. B **102,** 5947 (1998).
9. T. A. Alexander, P. M. Pellegrinol, and J. B. Gillespie, Appl. Spectrosc. **57,** 1340 (2003).
10. R. M. Jarvis and R. Goodacre, Anal Chem. **76,** 40 (2004).
11. G. J. Kovacs, R. O. Loutfy, and P. S. Vincent, Langmuir **2,** 689 (1986).
12. M. Moskovits, Rev. Modern Phys. **57,** 783 (1985).
13. E. Podstawka, Y. Ozaki, and L. M. Proniewicz, Appl. Spectrosc. **58,** 570 (2004).
14. K. Venkatakrishna, J. Kurien, K. M. Pai, M. Valiathan, N. N. Kumar, C. M. Krishna, G. Ullas, and V. B. Kartha, Curr. Sci. **80,** 665 (2001).
15. M. Moskovits and K. H. Michaelian, J. Chem. Phys. **69,** 2306 (1978).
16. K. Nakamoto, *Infrared and Raman Spectra of Inorganic and Coordination Compounds* (John Wiley and Sons, New York, 1986), 4th ed.
17. M. Kerker, O. Silman, L. A. Bumm, and D. S. Wang, Appl. Opt. **19,** 3253 (1980).
18. H. Wetzel and H. Gerischer, Chem. Phys. Lett. **76,** 460 (1980).
19. J. A. Creighton, C. G. Blatchford, and M. G. Albrecht, Faraday Trans. II **75,** 790 (1979).
20. J. Jiang, K. Bosnick, M. Maillard, and L. Brus, J. Phys. Chem. B **107,** 9964 (2003).
21. V. A. Markel, V. M. Shalev, P. Zhang, W. Huynh, L. Tay, T. L. Haslett, and M. Moskovits, Phys. Rev. B **59,** 10903 (1999).
22. A. Campion and P. Kambhampati, Chem. Soc. Rev. **27,** 241 (1998).
23. A. M. Michaels, J. Jiang, and L. Brus, J. Phys. Chem. B **104,** 11965 (2000).
24. H. Xu, E. J. Bjerneld, M. Käll, and L. Börjesson, Phys. Rev. Lett. **83,** 4357 (1999).
25. L. Zeiri, D. Sadler, B. V. Bronk, Y. Shabtai, J. Czégé, and S. Efrima, Colloids Surf. A **208,** 357 (2002).
26. X. Dou, Y. M. Jung, H. Yamamoto, S. Doi, and Y. Ozaki, Appl. Spectrosc. **53,** 133 (1999).
27. A. A. Ooka and R. L. Garell, Biopolymer (Biospectrosc.) **57,** 92 (2000).
28. Y. Zheng, P. R. Carey, and B. A. Palfey, J. Raman Spectrosc. **35,** 521 (2004).
29. K. C. Schuster, E. Urlaub, and J. R. Gapes, J. Microbiol. Methods **42,** 29 (2000).
30. H. Zhao, B. Yuan, and X. Dou, J. Opt. A: Pure Appl. Opt. **6,** 900 (2004).